Replication protein-A, RPA, plays a pivotal role in the maintenance of recombination checkpoint in yeast meiosis

Arivarasan Sampathkumar, Masaru Ito, Yurika Fujita, and Akira Shinohara*

Institute for Protein Research, Osaka University, Suita, Osaka 565-0871, Japan

Running title: Essential role of RPA in recombination checkpoint

Keywords: meiosis; homologous recombination; RPA; recombination checkpoint; Rfa1, auxin degron, synapsis checkpoint

*Corresponding author:
Akira Shinohara; ashino@protein.osaka-u.ac.jp

Lead contact:
Akira Shinohara
Institute for Protein Research, Osaka University,
3-2 Yamadaoka, Suita, Osaka 565-0871 JAPAN
Phone: 81-6-6879-8624
FAX: 81-6-6879-8626
E-mail: ashino@protein.osaka-u.ac.jp
ORCID: 0000-0003-4207-8247

Summary

DNA double-strand breaks (DSBs) activate DNA damage responses (DDR) in both mitotic and meiotic cells. Meiotic DSBs induce homologous recombination monitored by a meiotic DDR called the recombination checkpoint for the pachytene exit in meiotic prophase I. In this study, we showed the essential role of a single-stranded DNA (ssDNA) binding protein, Replication protein-A (RPA), in the maintenance of the recombination checkpoint during *S. cerevisiae* meiosis. The depletion of an RPA subunit, Rfa1, in a recombination-defective *dmc1* mutant, fully alleviates the pachytene arrest with the persistent unrepaired DSBs. RPA depletion downregulates a meiosis-specific CHK2 homolog, Mek1, which in turn activates Ndt80 transcriptional activator for pachytene exit. These support the idea that RPA is a sensor of ssDNAs for the activation of meiotic DDR. Rfa1 depletion also accelerates the prophase I delay induced by the *zip1* mutant defective in both chromosome synapsis and the recombination, suggesting that the accumulation of ssDNAs rather than defective synapsis triggers prophase I relay in the *zip1* mutant.

Introduction

A eukaryotic single-stranded (ss)DNA binding protein, Replication protein-A (RPA), plays an essential role in DNA replication, DNA repair, and homologous recombination [1-3]. RPA consists of three subunits; RPA70(RPA1), RPA32(RPA2), and RPA14(RPA3), which are highly conserved from yeast to humans. In *S. cerevisiae*, the knockout of three genes (*RFA1*, *-2* and *-3*) encoding the RPA subunits leads to lethality, consistent with its essential role in DNA replication [4].

DNA double-strand breaks (DSBs) initiate homologous recombination. RPA binds to ssDNA formed by the 5'-3' resection of the DSB ends to prevent the formation of the secondary structure of ssDNAs and to protect ssDNAs from degradation by various nucleases [5-7]. The assembly of Rad51 filaments on RPA-coated ssDNA is assisted by Rad51 mediators such as Rad52, Rad55-57, and Psy3-Csm2-Shu1-Shu2 in the budding yeast [8-10], and the Rad51 filament promotes homology search and strand exchange with a homologous double-stranded (ds)DNA [11,12]. The invasion of the ssDNA into the homologous dsDNA results in the formation of a displacement loop (D-loop). The 3'-OH end of the invading strand becomes a substrate for DNA synthesis. When a newly synthesized DNA strand is dissociated from the D-loop, the displaced ssDNA of the DSB end can capture the ssDNA of the other DSB end, which leads to a

gapped DNA for further second DNA synthesis. On the other hand, the stable association of the synthesized ssDNA with the D-loop results in the extension of the D-loop. The annealing of the displaced ssDNA with the ssDNA of the other DSB end results in the recombination intermediate with a Holliday structure. In these steps, RPA promotes DNA synthesis by DNA polymerases and the annealing between ssDNAs by Rad52 protein [13,14].

DNA damage activates the DNA damage response (DDR). DSB ends stimulate a DDR kinase, ATM/Tel1 (Ataxia telangiectasia mutated) while ssDSBs do an ATM homolog, ATR/Mec1 (Ataxia telangiectasia mutated related), both of which belong to the PI3 kinase family [15,16]. The activation of ATR is mediated by the interaction with an ATR partner, ATRIP/Ddc2, which directly binds to RPA [17-19]. In mammals, ATR activation is also mediated by the second RPA-binding protein, ETAA1 [20,21]. Thus, RPA is considered to work as an essential DNA damage sensor to detect ssDNAs, as well as a DNA damage processing protein. The Mec1/ATR activates downstream DDR responses such as DNA repair, cell-cycle arrest/delay, and/or apoptosis through a mediator kinase such as CHK2/Rad53.

Meiosis rewires DNA transactions such as homologous recombination/DSB repair as well as DDR response to guarantee the faithful segregation of two paternal homologous chromosomes at meiosis I for the reduction of chromosome numbers in gametes. In budding yeast, meiotic recombination is initiated by the DSB formation at recombination hotspots by the TopoVI-like protein, Spo11, which is followed by the formation of ssDNAs [22,23]. The ssDNA is used by a meiosis-specific Rad51 homolog, Dmc1 [24], for D-loop formation, which is aided by Rad51 [25] and its mediator, Mei5-Sae3 complex [26-28]. Further processing generates a recombination intermediate with double-Holliday junctions (dHJs), which are specifically resolved into crossovers between homologs. Importantly, the interhomolog bias for the partner choice in the recombination is mediated by meiosis-specific chromosome-axis proteins, Hop1-Red1-Mek1/Mre4, via an unknown mechanism [29-31]. Mek1/Mre4 (hereafter Mek1) kinase is a meiosis-specific homolog of Rad53/CHK2 kinase, which suppresses Rad51-mediated recombination in meiosis [32,33]. This suppression occurs through the Mek1-mediated phosphorylation of two proteins, Rad54 and Hed1 [34,35]. Rad54 belongs to the Swi2/Snf2 family protein essential for Rad51-mediated strand invasion [36,37]. Mek1-mediated phosphorylation of Rad54 suppresses its interaction with Rad51 [35]. Hed1, which is expressed only in meiosis, inhibits Rad51 by binding to the

Rad51-ssDNA complex [38]. The inhibitory activity of Hed1 against Rad51 and its protein stability are augmented by the Mek1 phosphorylation [34].

Meiotic events such as recombination and chromosome synapsis are strictly coupled with each other and also with meiosis progression (Figure 0) [39]. Similar to mitosis, DSBs in yeast meiosis activate Tel1(ATM) and Mec1(ATR). Different from mitotic DNA damage checkpoint, downstream events of Mec1 or Tel1 activation such as the Rad53 activation are largely suppressed in meiotic cells with poorly-defined mechanisms [40,41]. On the other hand, Mec1 and/or Tel1 phosphorylates a meiosis-specific chromosomal axis protein, Hop1 [42]. Mec1 activation is assisted by DDR clamp, Ddc1-Rad17-Mec1 (RAD9-RAD1-HUS1, 9-1-1 complex), and clamp loader, Rad24(RAD17) [42]. Together with chromosomal-bound Red1, phosphorylated Hop1 activates Mek1 kinase, whose autophosphorylation provides positive feedback on its activity [43]. Mek1-mediated phosphorylation promotes the inactivation of the Ndt80 transcription factor [44], which is essential for the exit from the mid-pachytene stage, where chromosome synapsis and the formation of the recombination intermediates with dHJs are completed [43,45]. By activating Ndt80 (inactivating Mek1), meiotic cells exit the pachytene stage by expressing downstream targets such as Cdc5 Polo-like kinase (PLK) and a cyclin, Clb1 [46] for the resolution of dHJs and the disassembly of the synaptonemal complex (SC), tripartite chromosome structure specific to meiosis.

It is widely believed that meiotic cells surveil not only homologous recombination but also chromosome synapsis (Figure 1). Like a recombination-defective *dmc1* mutant, the budding yeast *zip1* mutant, which is defective in the assembly of the central region of the SCs, thus synapsis, shows a delay in meiosis progression [47]. In nematodes and mice, synapsis-defective mutants also delay the meiotic prophase I progression and/or induce apoptosis [48,49]. However, in meiosis, chromosome synapsis is tightly coupled with meiotic recombination: e.g. a recombination-deficient mutant display also abnormal synapsis [50,51]; even the *zip1* mutant completely defective in SC formation impairs the processing of meiotic recombination intermediates. These complicate the presence of the synapsis checkpoint in meiotic cells. Moreover, genes involved in DDR response also play a role in meiotic recombination, which also provides a caveat in the interpretation of the meiotic phenotypes of DDR mutants [52,53].

Although the role of RPA in DDR response is widely accepted, the involvement *in vivo* remains unaddressed. A previous report showed that Rfa1

135 depletion in G2/M-arrested mitotic cells in budding yeast does not affect
136 checkpoint activation to a single DSB [5]. Moreover, the depletion of Rpa1 in mouse
137 spermatocytes eliminated RPA foci on meiotic chromosomes but is proficient in
138 ATR recruitment to the chromosomes [54]. These studies cast doubt on the role of
139 RPA in ATR-dependent checkpoint activation. In this study, we define the role of
140 RPA in the meiotic recombination checkpoint by using a conditional-depletion
141 mutant of Rfa1, RPA70 subunit of yeast RPA. The depletion of Rfa1 in the *dmc1*-
142 induced pachytene arrest facilitates the pachytene exits, thus entry into meiosis I
143 and II. Importantly, the RPA depletion accumulates meiotic DSBs without any
144 repair, which causes abnormal segregation of chromosomes in the division. This
145 confirms the essential role of RPA in the maintenance of the meiotic
146 recombination checkpoint. Moreover, we also found that Rfa1 depletion also
147 alleviates delayed meiosis progression in the *zip1* mutant, which is deficient in
148 SC formation and recombination. This suggests that the *zip1* mutation mainly
149 triggers an RPA-dependent response of the prophase delay, thus the
150 recombination checkpoint rather than the synapsis checkpoint.
151
152 **Results**
153 **Depletion of Rfa1 alleviates *dmc1*-induced arrest of meiosis**
154 The formation of ssDNA triggers cell cycle delay or arrest in both mitotic and
155 meiotic cells. To know the role of a major eukaryotic ssDNA-binding protein, RPA,
156 in the DNA damage-induced cell cycle arrest in budding yeast meiosis, we used
157 the *dmc1* mutant, which is unable to repair meiotic DSBs and as a result, an arrest
158 at mi-pachytene stage during meiotic prophase I [24]. This response to unrepaired
159 DSBs is referred to as the recombination checkpoint. Since all subunits of RPA,
160 Rfa1, -2, and -3, are essential for cell viability, we constructed a conditional
161 depletion mutant of the *RFA1* gene encoding the largest RPA subunit in the
162 budding yeast by the auxin-induced degron (AID) system. The AID tag was added
163 to the C-terminal of the Rfa1 protein. To know the role of RPA in the recombination
164 checkpoint in meiosis, *RFA1-AID* was introduced in the *dmc1* deletion mutant;
165 *dmc1 RFA1-AID*. Like the *dmc1* mutant, without auxin addition, *dmc1 RFA1-AID*
166 shows an arrest in meiotic prophase I without division (e.g. Figure 2B), indicating
167 that the Rfa1 tagging did not affect the recombination checkpoint in the absence
168 of Dmc1.
169 RPA is also involved in DNA replication and S-phase checkpoint [1,2], which
170 indirectly affects the G2 event. To avoid the effect in pre-meiotic DNA replication,

171 we depleted Rfa1 protein by adding auxin to a meiotic culture of *dmc1 RFA1-AID*
172 cells at 4 h after the induction of meiosis in the sporulation medium (SPM), after
173 pre-meiotic DNA replication, which occurs at 1.5-3 h. At 5 h, after the 1-hour
174 addition of auxin, the protein level of Rfa1-AID was decreased to ~15% level
175 relative to the original level at 4 h (Figure 2A), indicating the efficient depletion of
176 Rfa1 under the condition. We also checked the focus formation of Rfa2, the
177 second subunit of RPA, on meiotic chromosome spreads. Rfa2 shows punctate
178 staining on the spreads with other recombination proteins such as Rad51 [55],
179 which corresponds with ongoing recombination (Figure 2B). In the *dmc1* mutant,
180 Rfa2 focus-staining appears at 4 h, reaches a plateau at 5 h, and persists after
181 that, indicating little turnover of Rfa2 due to stalled recombination in the mutant
182 (Figure 2C, Supplemental Figure S1A). When auxin was added at 4 h, Rfa2 foci
183 disappeared within one hour (Figure 2A), and Rfa2 foci were rarely observed
184 during further incubation by 10 h (Figure 2B, C). This suggests that chromosome-
185 bound RPA is highly dynamic with an exchange of chromosome-bound ones with
186 that in a pool of nucleoplasm. We concluded that Rfa1 depletion at 4 h in meiosis
187 eliminates most chromosome-bound RPA complexes by 5 h.
188
189 **Checkpoint alleviation in Rfa1 depletion in *dmc1* meiosis**
190 DAPI staining of DNAs confirmed a single DAPI body in a *dmc1 RFA1-AID* cell
191 even at 24 h, thus an arrest in mid-pachynema, as shown previously [24]. Rfa1
192 depletion at 4 h induced fragmentation of DAPI bodies at late time points. In some
193 cells, 2-4 irregular-sized DAPI bodies with or without smaller DAPI bodies were
194 detected in a single cell (Figure 2D, top). The cells with abnormal DAPI bodies
195 appeared at 6 h and gradually accumulated by 24 h (Figure 2D, bottom). This
196 suggests the presence of nuclear division, thus the onset of meiosis I and/or II in
197 the *dmc1* cells upon Rfa1 depletion.
198 We also checked the effect of Rfa1 depletion on meiotic DNA replication.
199 The FACS analysis showed that the addition of auxin at 4 h did not affect the
200 transition from 2C to 4C (Figure 2E).
201 To evaluate the meiosis progression precisely, we examined the status of
202 spindle morphology in the *dmc1 RFA1-AID* cells in the absence or presence of
203 auxin (Figure 2F-H). Tubulin staining revealed a single focus associated with
204 single or multiple short projections in meiotic prophase I of the cell in the absence
205 of auxin (Figure 2G). The *dmc1 RFA1-AID* mutant maintained this arrangement
206 of spindles in the absence of auxin by 24 h, consistent with an arrest of the *dmc1*

207 mutant in prophase I (Figure 2H, left). On the other hand, the Rfa1 depletion
208 induced the elongation of spindles after one hour of addition (at 5 h). At 6 h, ~50%
209 *dmc1 RFA1-AID* cells contained single short and long spindles corresponding
210 with metaphase I and anaphase I, respectively (Figure 2H). At 8 h, in addition to
211 the metaphase I and anaphase I spindle, ~70% of cells contained metaphase II
212 or anaphase II spindles (Figure 2G). At 10 h, most of the cells showed diffuse
213 staining of microtubules in multiple DAPI bodies in a cell. These show that Rfa1
214 depletion almost alleviates meiotic prophase I arrest induced by the *dmc1*
215 mutation.
216 Cdc5/PLK is expressed after the pachytene exit [46]. Like *dmc1* cells, without
217 auxin addition, the *dmc1 RFA1-AID* mutant cells did not express Cdc5 (Figure
218 2A). On the other hand, the addition of auxin at 4 h induced the expression of
219 Cdc5 from 5 h. This confirms the exit of the pachytene stage of *dmc1* cells in the
220 absence of RPA.
221
222 **No DSB repair in *dmc1* meiosis with Rfa1 depletion**
223 One possibility to suppress the *dmc1* arrest is to channel unrepaired DSBs into
224 the repair pathway: e.g. the *rad51* mutation partially suppresses the *dmc1* arrest
225 [56,57]. On the other hand, the acute depletion of RPA did not affect the status of
226 meiotic DSBs. The CHEF gel electrophoresis confirmed the accumulation of
227 fragmented chromosomes in the *dmc1* mutant irrespective of the presence or
228 absence of RPA. In the *dmc1 RFA1-AID* mutant without auxin treatment, smear
229 bands of full-length chromosomes appeared at 3 h and most of the chromosomes
230 became fragmented with a size of less than 700 kbp by 5 h. After 6 h, fragmented
231 chromosomes persisted by 24 h (Figure 3A). The depletion of Rfa1 from 4 h did
232 not affect the persistence of fragmented chromosomes. This suggests that
233 meiotic DSBs remain unrepaired under the depletion of RPA in the *dmc1* mutant.
234 We also confirmed the DSB repair by immuno-staining analysis of Rad51
235 on meiotic chromosomes (Figure 3B, C). Like Rfa2 foci, in the *dmc1 RFA1-AID*
236 mutant in the absence of auxin, Rad51 foci appeared at 4 h, reached a plateau
237 at 5 h, and persisted at late times as shown previously [58]. The addition of auxin
238 at 4 h rapidly induced the disappearance of Rad51 foci at 5 h. The reduced Rad51
239 foci are seen at late time points (Figure 3C and Supplemental Figure 1B). This
240 suggests that RPA is critical for the maintenance of Rad51 foci on the
241 chromosomes. The absence of Rad51 foci in the Rfa1 depletion supports the
242 inability of *dmc1 RFA1-AID* cells without RPA to repair meiotic DSBs. Thus, RPA

243 might play an essential role in the post-synaptic stage of Rad51 assembly.
244
245 **The Hop1/Mek1-Ndt80 axis was down-regulated after RFA1 depletion**
246 Un-repaired DSBs in the *dmc1* mutant activate the recombination checkpoint,
247 which down-regulates a meiosis-specific transcription activator, Ndt80 for the
248 pachytene exit (Figure 1). DSB-activated Mec1/ATR kinase phosphorylates a
249 HORMAD protein, Hop1, which stimulates a meiosis-specific kinase, Mek1. Mek1
250 binds and phosphorylates Ndt80 to inactivate it. For pachytene exit, further
251 phosphorylation of Nd80 by Ime2 kinase promotes the activation of Ndt80 [59]. In
252 *dmc1 RFA1-AID* cells, the Ndt80 appeared at 4 h with multiple bands and
253 accumulated more during further incubation in SPM without a change of band-
254 shift status (Figure 2A). At 6 h, after two hours of addition of auxin, a slower-
255 migrating Ndt80 band appeared and gradually decreased in intensity. Importantly,
256 as shown above, under the depletion condition, Cdc5/PLK, which is a major target
257 of activated Ndt80 and is necessary for pachytene exit, appeared at 6 h (Figure
258 2A). This is consistent with meiosis progression induced by Rfa1-depletion as
259 shown above.
260 We also checked the behavior of the upstream regulators of Ndt80, Hop1,
261 and Mek1 by western blotting. In the *dmc1* mutant, Hop1 appeared as a non-
262 phosphorylated form at 2 h and phosphorylated Hop1 with slower migrated bands
263 by Mec1(ATR) or Tel1(ATM) persisted from 4 h (Figure 2A) as shown previously
264 [42]. After Rfa1 depletion, major bands of phosphorylated Hop1 almost disappeared
265 from 6 h with a similar steady-state level of non-phosphorylated Hop1 during the
266 time course. This suggests that Hop1 phosphorylation is actively de-
267 phosphorylated during pachytene exit. On chromosome spreads, Hop1 shows
268 beads-in-line staining for the localization of chromosome axes (Figure 3D) [60,61].
269 In the *dmc1* mutant without Rfa1 depletion, Hop1 localization remains unchanged
270 during meiosis (Figure 3D). The addition of auxin at 4 h induced the
271 disappearance of Hop1-positive spreads from 5 h. At 6 h, ~35% of cells are
272 positive for Hop1 while ~95% are positive in a control (Figure 3D, E). At 8 h, most
273 of the Hop1 signals on the chromosomes disappeared.
274 One of the Mek1 kinase targets is histone H3T11 phosphorylation [62]. Under
275 the *dmc1* arrest condition, H3T11 phosphorylation accumulated (Figure 2A). On
276 the other hand, the Rfa1 depletion rapidly induced the disappearance of the
277 signal (Figure 2A), suggesting the inactivation of Mek1 under Rfa1 depletion.
278 These results clearly showed that Rfa1, thus RPA, is critical for the maintenance

279 of the recombination checkpoint through the Hop1/Mek1-Ndt80 axis.
280
281 **Bypass of *dmc1* arrest by Rfa1 depletion depends on Ndt80**
282 We confirmed whether the pachytene exit of the *dmc1* cells by Rfa1 depletion
283 depends on the *NDT80* (Figure 4). The addition of auxin to *dmc1 ndt80 RFA1-*
284 *AID* cells efficiently reduced the amount of Rfa1 protein (Figure 4A) and Rfa2 foci
285 from meiotic chromosomes (Figure 4B). However, different from the *dmc1 RFA1-*
286 *AID* mutant, the addition of auxin to *dmc1 ndt80 RFA1-AID* mutant did not induce
287 the elongation of spindles (Figure 4C) or Hop1 disassembly from the
288 chromosomes (Figure 4D). Thus, the pachytene exit of *dmc1* cells by Rfa1
289 depletion still depends on Ndt80. Interestingly, the amount of the phosphorylated
290 Hop1 is reduced slightly compared to that in the control (Figure 4A). This is not
291 drastic compared to the presence of Ndt80, supporting an auto-feedback
292 mechanism between Mec1 activation and Ndt80 activation [63]. Moreover, the
293 Hop1 dephosphorylation is not a prerequisite for Hop1 dissociation from meiotic
294 chromosomes.
295
296 **Checkpoint alleviation in Rfa1 depletion in *zip1* meiosis**
297 Meiotic yeast cells monitor not only ongoing meiotic recombination but also
298 chromosome synapsis [49]. However, the presence of the so-called "synapsis
299 checkpoint" is under debate [63]. The mutant in the *ZIP1* gene, which encodes the
300 transverse filament of the central region of the SC [47], is deficient in chromosome
301 synapsis with a delay of the entry into meiosis I and is used to analyze the
302 synaptic checkpoint. We examined the effect of Rfa1 depletion on the *zip1-*
303 induced delay of meiosis I (Figure 5). As reported previously [51], in the SK1 strain
304 background, *zip1 RFA1-AID* cells without auxin addition started meiosis I at 8 h
305 while wild-type cells entered at 5 h (and finished meiosis II by 10 h) (Figure 5B).
306 When auxin was added at 4 h, which induced rapid depletion of Rfa1 and the
307 dissociation of Rfa2 from meiotic chromosomes (Figure 5A, C, I), metaphase I
308 spindles appeared at 5 h, and at 6 h, ~35% of the cells contained metaphase-I
309 and anaphase-I spindles (Figure 5D, E). At 8 h, ~30% of the cells contained
310 anaphase-II spindle. However, compared to the control, the entry into meiosis I
311 and II is not efficient.
312 The *zip1 RFA1-AID* cells without auxin expressed Cdc5 from 8 h (Figure
313 5A), consistent with delayed progression of prophase I in the mutant. The addition
314 of auxin at 4 h accelerated the Cdc5 expression at 5 h. The *zip1* mutant

accumulated T11 phosphorylation of histone H3 signal from 4 h to 8 h (Figure 5A). The Rfa1 depletion accelerated the disappearance of this phosphorylation from 5 h. The accelerated disappearance of the phosphor-Hop1 protein is also seen by the depletion. These showed the Rfa1-dependent inactivation of the Hop1/Mek1-Ndt80 signaling pathway induced by the *zip1* mutation. Thus, the delay induced by the *zip1* mutation largely depends on the Rfa1 function.

In addition to SC formation, Zip1 plays a critical role in meiotic recombination as a pro-CO factor. Indeed, the *zip1* mutant shows delayed DSB repair. The CHEF analysis showed the presence of broken chromosomes in the *zip1* mutant from 3 h to 8 h (Figure 5H). Importantly, full-length chromosomes were reassembled at 10 h without Rfa1 depletion, indicating that most of the DSBs in the mutant are repaired with the delay. On the other hand, Rfa1 depletion from 4 h induced fragmentation of the chromosomes from 5 h. Even after 24 h, little recovery of full-length chromosomes was seen under the condition. This suggests that Rfa1 is essential for meiotic DSB repair in the *zip1* mutant.

Rfa1 depletion does not alleviate delay induced by *rad50S* meiosis

The *rad50S* mutant, which is defective in the end-processing of meiotic DSBs, also shows delayed meiosis I progression [64]. This delay in the *rad50S* mutant is mediated by Tel1(ATM) and Rad50-Mre11-Xrs2, which recognize DSB ends [65]. The pathway is distinct from the Mec1(ATR)-mediated pathway shown above. We also examined the effect of Rfa1 depletion on the *rad50S*-induced delay (Figure 6). As reported, without auxin, *rad50S RFA1-AID* cells with auxin addition delay the onset of meiosis I as shown by whole-cell staining of tubulin (Figure 6B). Rather, the addition of auxin delayed the onset of meiosis I induced by the *rad50S* mutation. We cannot detect Rfa2 foci in the r*ad50S* mutant even in the presence of Rfa1 (Figure 6C), which accumulates DSBs in late meiosis I as shown by the CHEF analysis (Figure 6D). The Rfa1 depletion did not affect the kinetics of the accumulation of chromosome fragments (Figure 6D). Moreover, Hop1 phosphorylation is not observed in the mutant (Figure 6A). This is consistent with little formation of ssDNAs without DSB processing in the mutant [64], thus little Mec1/ATR activation. This is not surprising since the *rad50S* mutant does not form any ssDNAs, which is a substrate for RPA. The accumulation of chromosomal Hop1 in the mutant is not affected by the Rfa1 depletion (Figure 6E).

351 **Discussion**

352 RPA plays multiple roles in DNA replication, DNA repair, and recombination
353 through its ability to bind to ssDNAs with a high affinity. RPA is also important for
354 DDR as a sensor of DNA damage, thus ssDNAs. Although the role of RPA in
355 Mec1/ATR activation through the binding of Mec1/ATR-interaction protein,
356 Ddc1(ATRIP), to RPA has been documented well [17,18,66], the *in vivo* evidence to
357 support the role of RPA as the DDR sensor is still missing. In this paper, we
358 showed the pivotal role of RPA in the maintenance of DDR in meiosis, called
359 recombination checkpoint.

360

361 **The role of RPA in recombination checkpoint**

362 Although the role of RPA on ssDNA for the recruitment of Mec1-Ddc2(ATR-
363 ATRIP) for Mec1/ATR-activation in the DDR response is well-established [17,18,66],
364 There is no provided *in vivo* evidence that RPA acts as an ssDNA sensor.
365 Previously, in the budding yeast, two *RFA1*-degron mutants, *rfa1-td* and *td-RFA1*,
366 were constructed and characterized to study the role of Rfa1 in DDR activation.
367 Indeed, the *rfa1-td*, as well as the *rft1-t11 (rfa1-K45E)* mutant, reduce the
368 recruitments of Ddc2 to a DSB site [66]. On the other hand, it is shown that, by
369 using the *td-RFA1*, G2/M-arrested haploid cells depleted Rfa1 still activate Rad53
370 upon a single DSB [5]. The latter study concludes that a low level of RPA is
371 sufficient for the activation of Mec1-Ddc2. More recently, an RPA-independent
372 pathway for ATR activation, which requires APE1, was identified in *Xenopus*
373 extracts [67]. We evaluated the role of RPA in DDR activation by studying the effect
374 of Rfa1 depletion in the meiotic recombination checkpoint which shares the Mec1-
375 dependent DDR pathway with a canonical DNA damage checkpoint in yeast
376 mitotic cells. By using the auxin-degron, we depleted Rfa1 in the *dmc1* mutant
377 which arrests in meiotic prophase I with hyper-resected ssDNAs in ~150 DSBs
378 [24]. As expected, the Rfa1-depletion induced the pachytene exit by downregulating
379 Mec1-Mek1 activity, which in turn activates the Ndt80-dependent gene
380 expression of key regulators for the pachytene exit such as Cdc5 [43]. Importantly,
381 the Rfa1 depletion did not affect the accumulation of ssDNAs in the *dmc1* cells
382 with persistent unrepaired DSBs. This is particularly important since mutations in
383 DDR genes such as *RAD17*, *-24*, *DDC1*, and *MEC3* even in the *MEC1* gene
384 bypass the *dmc1*-induced arrest by activating the other DSB repair pathway such
385 as ectopic recombination [52,53,68]. The results described here provide strong *in vivo*
386 evidence that RPA is a sensor for ssDNAs, which creates a scaffold for the

assembly of checkpoint effectors assembly such as Mec1-Ddc1(ATR-ATRIP). In meiosis, rather than activating Rad53 kinase, a meiosis-specific Mek1 is activated through the phosphorylation of Hop1 by Mec1 kinase[42]. The Rfa1-depletion induces rapid dephosphorylation of Hop1 and the dissociation from meiotic chromosomes without affecting the protein level, suggesting the presence of active de-phosphorylation, probably by Mec1-bound phosphatase, PP4 [69,70].

The chromosome synapsis checkpoint in yeast meiosis

In addition to the recombination checkpoint, meiotic cells show a response to abnormal chromosome synapsis called synapsis checkpoint. This idea was proposed that mutants defective in chromosome synapsis show a delay in the progression of prophase I and apoptosis in yeasts and mice, respectively. However, the presence of the synapsis checkpoint is still under debate [48,49], since in most organisms meiotic recombination and chromosome synapsis are tightly coupled. The budding yeast *zip1* mutant, which is completely defective in SC formation, thus, chromosome synapsis, delays or arrest in meiotic prophase I [47,51]. This arrest is alleviated by the mutant of genes encoding a component of checkpoint such as *PCH2* [71]. Pch2 modulates Hop1 conformation and regulates the association and dissociation of Hop1 on meiotic chromosomes [56,72,73]. On the other hand, the *zip1* mutant also shows defective DSB repair and/or the crossing-over [50,51], which suggests delayed progression of meiosis I in the *zip1* mutant is caused by the impaired recombination. In this study, by using the *RFA1-AID*, we could test whether the delay in *zip1* mutant depends on RPA or not and found that the Rfa1-depletion eliminates the delay induced by the *zip1* mutation. This strongly suggests that the recombination checkpoint delays the meiosis I progression in the *zip1* mutant as seen in the *dmc1* mutant. Moreover, consistent with this, the other yeast mutants, which are defective in the synapsis with normal recombination such as *ecm11* and *gmc2*, do not show a drastic delay in the meiosis I progression [74,75]. Thus, at least in budding yeast which couples the recombination and chromosome synapsis, rather than the status of chromosome synapsis, a recombination process, the presence of ssDNAs, can be monitored by a meiosis-specific surveillance mechanism to guarantee the completion of meiotic recombination directly and chromosome synapsis indirectly.

Materials and Methods

Strains and plasmids

423 All strains described here are derivatives of *S. cerevisiae* SK1 diploids,
424 NKY832/833 (*MATα/MAT**a**, lys2/", ura3/", leu2::hisG/", trp1::hisG/"*). The
425 genotypes of each strain used in this study are described in Supplementary Table
426 S1.
427
428 **Strain Construction**
429 The *RFA1-AID* gene was constructed by one-step DNA integration using a
430 template plasmid, which was provided by Dr. Neil Hunter, with primers shown in
431 Table S2. DNA changes were confirmed by DNA sequencing.
432
433 **Anti-serum and antibodies**
434 Anti-myc (Santa Cruz), anti-tubulin (MCA77G, Bio-Rad/Serotec, Ltd), anti-Cdc5
435 (Santa Cruz), and histone H3 phospho-T11 (Abcam) were used for western
436 blotting. Rabbit anti-Rad51 [25] and guinea pig anti-Rad51 [76], rabbit anti-Hop1 and
437 rabbit anti-Rfa2 were used for staining. Rabbit anti-Ndt80 was a gift by M. Lichten.
438 The secondary antibodies for immuno-staining were Alexa Fluor 488 (Goat) and
439 594 (Goat) IgG used at a 1/2000 dilution (Thermo Fisher Scientific). For western
440 blotting, alkaline phosphatase-conjugated secondary antibodies (Promega) were
441 used.
442
443 **Meiotic Time course**
444 *Saccharomyces cerevisiae* SK1 strains were patched onto YPG plates (2%
445 bacteriological peptone, 1% yeast extract, 3% glycerol, 2% bacteriological agar)
446 and incubated at 30 °C for 12 h. Cells were inoculated onto YPD plates (2%
447 bacteriological peptone, 1% yeast extract, 2% glucose, 2% bacteriological agar)
448 and grown for two days to obtain isolated colonies. A single colony was inoculated
449 into 3 ml of YPD liquid medium and grown to saturation at 30 °C overnight. To
450 synchronize cell cultures, the overnight cultures were transferred to pre-warmed
451 SPS medium (1% potassium acetate, 1% bacteriological peptone, 0.5% yeast
452 extract, 0.17% yeast nitrogen base with ammonium sulfate and without amino
453 acids, 0.5% ammonium sulfate, 0.05 M potassium biphthalate) and grown for 16–
454 17 h. Meiosis was induced by transferring the SPS-cultured cells to pre-warmed
455 SPM (1% potassium acetate, 0.02% raffinose). The SPM-cultured cells were
456 harvested at various times after transfer. Auxin was added at a final concentration
457 of 4 mM.
458

459 **Cytology**
460 Chromosome spreads were immunostained as described previously [53,76].
461 Spheroplasts were burst in the presence of 1% paraformaldehyde and 0.1% lipsol.
462 Stained samples were stained with primary and secondary antibodies observed
463 using a fluorescence microscope (BX51; Olympus/Evident) with a 100× objective
464 (NA1.3). Images were captured by CCD camera (CoolSNAP; Roper), and then
465 processed using IP lab and/or iVision (Bio Vision Technologies) and Photoshop
466 (Adobe) software. For focus counting, ~30 nuclei were counted at each time point.
467 Whole-cell staining was carried out as follows. Yeast cells are fixed with
468 formaldehyde (3.7%) and placed on a glass slide coated with poly-lysine. The
469 cells were treated with cold ethanol and acetone and stained with primary and
470 secondary antibodies.
471
472 **Western blotting**
473 Western blotting was performed as described previously [27,77] , using cell lysates
474 extracted by the TCA method. After being harvested and washed twice with 20%
475 TCA, cells were roughly disrupted with zirconia beads by the Multi-beads shocker
476 (Yasui Kikai). The protein precipitate recovered by centrifugation was suspended
477 in SDS-PAGE sample buffer adjusted to pH 8.8 and then incubated at 95 °C for
478 10 min. After electrophoresis, the proteins were transferred onto a nylon
479 membrane (Immobilon-P, Millipore) and incubated with primary antibodies in a
480 blocking buffer (1× PBS, 0.5% BSA) and then with alkaline phosphatase-
481 conjugated secondary antibody (Promega). The color reaction was developed
482 with NBT/BCIP solution (Nacalai Tesque).
483
484 **CHEF analysis Pulsed-field gel electrophoresis**
485 For pulsed-field gel electrophoresis (PFGE), chromosomal DNA was prepared in
486 agarose plugs as described in [78] and run at 14 °C in a CHEF DR-III apparatus
487 (BioRad) using the field 6V/cm at a 120° angle. Switching times followed a ramp
488 from 15.1 to 25.1 seconds. Duration of electrophoresis was 41 h for chromosome
489 III.
490
491 **FACS analysis**
492 Cells in 1 ml of SPM culture were collected by centrifugation. The pellet was then
493 resuspended in 1 ml of 70% ethanol. Fixed cells were recollected and washed by
494 suspending 1 ml of 50 mM sodium citrate buffer. The collected cells were

resuspended in 0.5 ml of sodium citrate buffer and sonicated for the 20s at room temperature. Sonicated cells were incubated with 12.5 μl of 10 mg/mL RNAseA for 1 h at 50 °C and in 25 μl of 15mg/ml proteinase K for 1h at 50 °C. 0.5ml of 16 μlg/mL PI solution was added and incubated for 30 min at room temperature in the dark. The samples were then analyzed using SA-3800 Spectral analyzer (Sony). Floreada.io was used for gating and plotting graphs.

Statistics

Means ± S.D values are shown. Datasets were compared using the Mann-Whitney U-test. χ^2-test was used for proportion. Multiple test correction was done with Bonferroni's correction. *, **, and *** show *P*-values of <0.05, <0.01 and <0.001, respectively.

Acknowledgments

We are grateful to Drs. Neil Hunter for providing the yeast AID system and Michael Lichten for anti-Ndt80. A.Sa. is a JICA fellow. Y.F. and M.I. were supported by the Institute for Protein Research. This work was supported by a grant from Institute for Fermentation, Osaka (IFO) and from Uehara Memorial Foundation to Life Sciences; to A.Sh.

Competing interest

The authors declare no competing financial interest.

Author contributions

A.Sh. conceived and designed the experiments. A.Sa. carried out experiments with help from Y.F. and M.I.. A.Sa, Y.F., M.I., and A.Sh. analyzed the data. A.Sh. wrote the manuscript with inputs from help from others.

524 **References**

525

526 1 Bhat, K. P. & Cortez, D. RPA and RAD51: fork reversal, fork protection,
527 and genome stability. *Nat Struct Mol Biol* **25**, 446-453 (2018).
528 https://doi.org:10.1038/s41594-018-0075-z

529 2 Caldwell, C. C. & Spies, M. Dynamic elements of replication protein A at
530 the crossroads of DNA replication, recombination, and repair. *Crit Rev*
531 *Biochem Mol Biol* **55**, 482-507 (2020).
532 https://doi.org:10.1080/10409238.2020.1813070

533 3 Wold, M. S. Replication protein A: a heterotrimeric, single-stranded DNA-
534 binding protein required for eukaryotic DNA metabolism. *Annu Rev*
535 *Biochem* **66**, 61-92 (1997).
536 https://doi.org:10.1146/annurev.biochem.66.1.61

537 4 Brill, S. J. & Stillman, B. Replication factor-A from Saccharomyces
538 cerevisiae is encoded by three essential genes coordinately expressed at
539 S phase. *Genes Dev* **5**, 1589-1600 (1991).
540 https://doi.org:10.1101/gad.5.9.1589

541 5 Chen, H., Lisby, M. & Symington, L. S. RPA coordinates DNA end resection
542 and prevents formation of DNA hairpins. *Mol Cell* **50**, 589-600 (2013).
543 https://doi.org:10.1016/j.molcel.2013.04.032

544 6 Deng, S. K., Chen, H. & Symington, L. S. Replication protein A prevents
545 promiscuous annealing between short sequence homologies: Implications
546 for genome integrity. *Bioessays* **37**, 305-313 (2015).
547 https://doi.org:10.1002/bies.201400161

548 7 Ruff, P., Donnianni, R. A., Glancy, E., Oh, J. & Symington, L. S. RPA
549 Stabilization of Single-Stranded DNA Is Critical for Break-Induced
550 Replication. *Cell Rep* **17**, 3359-3368 (2016).
551 https://doi.org:10.1016/j.celrep.2016.12.003

552 8 Sasanuma, H. *et al.* A new protein complex promoting the assembly of
553 Rad51 filaments. *Nat Commun* **4**, 1676 (2013).
554 https://doi.org:10.1038/ncomms2678

555 9 Shinohara, A. & Ogawa, T. Stimulation by Rad52 of yeast Rad51-mediated
556 recombination. *Nature* **391**, 404-407 (1998). https://doi.org:10.1038/34943

557 10 Sung, P. Yeast Rad55 and Rad57 proteins form a heterodimer that
558 functions with replication protein A to promote DNA strand exchange by
559 Rad51 recombinase. *Genes Dev* **11**, 1111-1121 (1997).

560 https://doi.org:10.1101/gad.11.9.1111
561 11 Sung, P. Catalysis of ATP-dependent homologous DNA pairing and strand
562 exchange by yeast RAD51 protein. *Science* **265**, 1241-1243 (1994).
563 https://doi.org:10.1126/science.8066464
564 12 Sung, P. & Robberson, D. L. DNA strand exchange mediated by a RAD51-
565 ssDNA nucleoprotein filament with polarity opposite to that of RecA. *Cell*
566 **82**, 453-461 (1995). https://doi.org:10.1016/0092-8674(95)90434-4
567 13 Shinohara, A., Shinohara, M., Ohta, T., Matsuda, S. & Ogawa, T. Rad52
568 forms ring structures and co-operates with RPA in single-strand DNA
569 annealing. *Genes Cells* **3**, 145-156 (1998). https://doi.org:10.1046/j.1365-
570 2443.1998.00176.x
571 14 Sugiyama, T., New, J. H. & Kowalczykowski, S. C. DNA annealing by
572 RAD52 protein is stimulated by specific interaction with the complex of
573 replication protein A and single-stranded DNA. *Proceedings of the National*
574 *Academy of Sciences of the United States of America* **95**, 6049-6054
575 (1998). https://doi.org:10.1073/pnas.95.11.6049
576 15 Friedel, A. M., Pike, B. L. & Gasser, S. M. ATR/Mec1: coordinating fork
577 stability and repair. *Curr Opin Cell Biol* **21**, 237-244 (2009).
578 https://doi.org:10.1016/j.ceb.2009.01.017
579 16 Williams, R. M., Yates, L. A. & Zhang, X. Structures and regulations of ATM
580 and ATR, master kinases in genome integrity. *Curr Opin Struct Biol* **61**, 98-
581 105 (2020). https://doi.org:10.1016/j.sbi.2019.12.010
582 17 Biswas, H., Goto, G., Wang, W., Sung, P. & Sugimoto, K. Ddc2ATRIP
583 promotes Mec1ATR activation at RPA-ssDNA tracts. *PLoS Genet* **15**,
584 e1008294 (2019). https://doi.org:10.1371/journal.pgen.1008294
585 18 Deshpande, I. *et al.* Structural Basis of Mec1-Ddc2-RPA Assembly and
586 Activation on Single-Stranded DNA at Sites of Damage. *Mol Cell* **68**, 431-
587 445 e435 (2017). https://doi.org:10.1016/j.molcel.2017.09.019
588 19 Yates, L. A., Tannous, E. A., Morgan, R. M., Burgers, P. M. & Zhang, X. A
589 DNA damage-induced phosphorylation circuit enhances Mec1(ATR)
590 Ddc2(ATRIP) recruitment to Replication Protein A. *Proceedings of the*
591 *National Academy of Sciences of the United States of America* **120**,
592 e2300150120 (2023). https://doi.org:10.1073/pnas.2300150120
593 20 Bass, T. E. *et al.* ETAA1 acts at stalled replication forks to maintain genome
594 integrity. *Nat Cell Biol* **18**, 1185-1195 (2016).
595 https://doi.org:10.1038/ncb3415

596 21 Haahr, P. *et al.* Activation of the ATR kinase by the RPA-binding protein
597 ETAA1. *Nat Cell Biol* **18**, 1196-1207 (2016).
598 https://doi.org:10.1038/ncb3422
599 22 Bergerat, A. *et al.* An atypical topoisomerase II from Archaea with
600 implications for meiotic recombination. *Nature* **386**, 414-417 (1997).
601 https://doi.org:10.1038/386414a0
602 23 Keeney, S., Giroux, C. N. & Kleckner, N. Meiosis-specific DNA double-
603 strand breaks are catalyzed by Spo11, a member of a widely conserved
604 protein family. *Cell* **88**, 375-384 (1997).
605 24 Bishop, D. K., Park, D., Xu, L. & Kleckner, N. DMC1: a meiosis-specific
606 yeast homolog of E. coli recA required for recombination, synaptonemal
607 complex formation, and cell cycle progression. *Cell* **69**, 439-456 (1992).
608 25 Shinohara, A., Ogawa, H. & Ogawa, T. Rad51 protein involved in repair
609 and recombination in S. cerevisiae is a RecA-like protein. *Cell* **69**, 457-470
610 (1992).
611 26 Cloud, V., Chan, Y. L., Grubb, J., Budke, B. & Bishop, D. K. Rad51 is an
612 accessory factor for Dmc1-mediated joint molecule formation during
613 meiosis. *Science* **337**, 1222-1225 (2012).
614 https://doi.org:10.1126/science.1219379
615 27 Hayase, A. *et al.* A protein complex containing Mei5 and Sae3 promotes
616 the assembly of the meiosis-specific RecA homolog Dmc1. *Cell* **119**, 927-
617 940 (2004).
618 28 Tsubouchi, H. & Roeder, G. S. The budding yeast mei5 and sae3 proteins
619 act together with dmc1 during meiotic recombination. *Genetics* **168**, 1219-
620 1230 (2004). https://doi.org:10.1534/genetics.103.025700
621 29 Hong, S. *et al.* The logic and mechanism of homologous recombination
622 partner choice. *Mol Cell* **51**, 440-453 (2013).
623 https://doi.org:10.1016/j.molcel.2013.08.008
624 30 Kim, K. P. *et al.* Sister cohesion and structural axis components mediate
625 homolog bias of meiotic recombination. *Cell* **143**, 924-937 (2010).
626 https://doi.org:10.1016/j.cell.2010.11.015
627 31 Niu, H. *et al.* Partner choice during meiosis is regulated by Hop1-promoted
628 dimerization of Mek1. *Molecular biology of the cell* **16**, 5804-5818 (2005).
629 https://doi.org:10.1091/mbc.e05-05-0465
630 32 Leem, S. H. & Ogawa, H. The MRE4 gene encodes a novel protein kinase
631 homologue required for meiotic recombination in Saccharomyces

632 cerevisiae. *Nucleic Acids Res* **20**, 449-457 (1992).
633 https://doi.org:10.1093/nar/20.3.449
634 33 Rockmill, B. & Roeder, G. S. A meiosis-specific protein kinase homolog
635 required for chromosome synapsis and recombination. *Genes Dev* **5**,
636 2392-2404 (1991). https://doi.org:10.1101/gad.5.12b.2392
637 34 Callender, T. L. *et al.* Mek1 Down Regulates Rad51 Activity during Yeast
638 Meiosis by Phosphorylation of Hed1. *PLoS Genet* **12**, e1006226 (2016).
639 https://doi.org:10.1371/journal.pgen.1006226
640 35 Niu, H. *et al.* Regulation of meiotic recombination via Mek1-mediated
641 Rad54 phosphorylation. *Mol Cell* **36**, 393-404 (2009).
642 https://doi.org:10.1016/j.molcel.2009.09.029
643 36 Jiang, H. *et al.* Direct association between the yeast Rad51 and Rad54
644 recombination proteins. *J Biol Chem* **271**, 33181-33186 (1996).
645 https://doi.org:10.1074/jbc.271.52.33181
646 37 Petukhova, G., Stratton, S. & Sung, P. Catalysis of homologous DNA
647 pairing by yeast Rad51 and Rad54 proteins. *Nature* **393**, 91-94 (1998).
648 https://doi.org:10.1038/30037
649 38 Tsubouchi, H. & Roeder, G. S. Budding yeast Hed1 down-regulates the
650 mitotic recombination machinery when meiotic recombination is impaired.
651 *Genes Dev* **20**, 1766-1775 (2006). https://doi.org:10.1101/gad.1422506
652 39 Borner, G. V., Hochwagen, A. & MacQueen, A. J. Meiosis in budding yeast.
653 *Genetics* (2023). https://doi.org:10.1093/genetics/iyad125
654 40 Cartagena-Lirola, H., Guerini, I., Manfrini, N., Lucchini, G. & Longhese, M.
655 P. Role of the Saccharomyces cerevisiae Rad53 checkpoint kinase in
656 signaling double-strand breaks during the meiotic cell cycle. *Molecular and*
657 *cellular biology* **28**, 4480-4493 (2008).
658 https://doi.org:10.1128/MCB.00375-08
659 41 Usui, T. & Shinohara, A. Rad9, a 53BP1 Ortholog of Budding Yeast, Is
660 Insensitive to Spo11-Induced Double-Strand Breaks During Meiosis. *Front*
661 *Cell Dev Biol* **9**, 635383 (2021). https://doi.org:10.3389/fcell.2021.635383
662 42 Carballo, J. A., Johnson, A. L., Sedgwick, S. G. & Cha, R. S.
663 Phosphorylation of the axial element protein Hop1 by Mec1/Tel1 ensures
664 meiotic interhomolog recombination. *Cell* **132**, 758-770 (2008).
665 https://doi.org:10.1016/j.cell.2008.01.035
666 43 Hollingsworth, N. M. Mek1/Mre4 is a master regulator of meiotic
667 recombination in budding yeast. *Microb Cell* **3**, 129-131 (2016).

668 https://doi.org:10.15698/mic2016.03.487
669 44 Xu, L., Ajimura, M., Padmore, R., Klein, C. & Kleckner, N. NDT80, a
670 meiosis-specific gene required for exit from pachytene in Saccharomyces
671 cerevisiae. *Molecular and cellular biology* **15**, 6572-6581 (1995).
672 https://doi.org:10.1128/MCB.15.12.6572
673 45 Hochwagen, A. Meiosis: making a synaptonemal complex just got easier.
674 *Curr Biol* **19**, R849-851 (2009). https://doi.org:10.1016/j.cub.2009.07.001
675 46 Sourirajan, A. & Lichten, M. Polo-like kinase Cdc5 drives exit from
676 pachytene during budding yeast meiosis. *Genes Dev* **22**, 2627-2632
677 (2008). https://doi.org:10.1101/gad.1711408
678 47 Sym, M., Engebrecht, J. A. & Roeder, G. S. ZIP1 is a synaptonemal
679 complex protein required for meiotic chromosome synapsis. *Cell* **72**, 365-
680 378 (1993).
681 48 Huang, Y. & Roig, I. Genetic control of meiosis surveillance mechanisms
682 in mammals. *Front Cell Dev Biol* **11**, 1127440 (2023).
683 https://doi.org:10.3389/fcell.2023.1127440
684 49 MacQueen, A. J. & Hochwagen, A. Checkpoint mechanisms: the puppet
685 masters of meiotic prophase. *Trends Cell Biol* **21**, 393-400 (2011).
686 https://doi.org:10.1016/j.tcb.2011.03.004
687 50 Borner, G. V., Kleckner, N. & Hunter, N. Crossover/noncrossover
688 differentiation, synaptonemal complex formation, and regulatory
689 surveillance at the leptotene/zygotene transition of meiosis. *Cell* **117**, 29-
690 45 (2004).
691 51 Storlazzi, A., Xu, L., Schwacha, A. & Kleckner, N. Synaptonemal complex
692 (SC) component Zip1 plays a role in meiotic recombination independent
693 of SC polymerization along the chromosomes. *Proceedings of the National*
694 *Academy of Sciences of the United States of America* **93**, 9043-9048
695 (1996). https://doi.org:10.1073/pnas.93.17.9043
696 52 Grushcow, J. M. *et al.* Saccharomyces cerevisiae checkpoint genes MEC1,
697 RAD17 and RAD24 are required for normal meiotic recombination partner
698 choice. *Genetics* **153**, 607-620 (1999).
699 https://doi.org:10.1093/genetics/153.2.607
700 53 Shinohara, M., Sakai, K., Ogawa, T. & Shinohara, A. The mitotic DNA
701 damage checkpoint proteins Rad17 and Rad24 are required for repair of
702 double-strand breaks during meiosis in yeast. *Genetics* **164**, 855-865
703 (2003). https://doi.org:10.1093/genetics/164.3.855

704 54 Shi, B. *et al.* Dual functions for the ssDNA-binding protein RPA in meiotic
705 recombination. *PLoS Genet* **15**, e1007952 (2019).
706 https://doi.org:10.1371/journal.pgen.1007952
707 55 Gasior, S. L., Wong, A. K., Kora, Y., Shinohara, A. & Bishop, D. K. Rad52
708 associates with RPA and functions with rad55 and rad57 to assemble
709 meiotic recombination complexes. *Genes Dev* **12**, 2208-2221 (1998).
710 https://doi.org:10.1101/gad.12.14.2208
711 56 Raina, V. B. & Vader, G. Homeostatic Control of Meiotic Prophase
712 Checkpoint Function by Pch2 and Hop1. *Curr Biol* **30**, 4413-4424 e4415
713 (2020). https://doi.org:10.1016/j.cub.2020.08.064
714 57 Shinohara, A., Gasior, S., Ogawa, T., Kleckner, N. & Bishop, D. K.
715 Saccharomyces cerevisiae recA homologues RAD51 and DMC1 have
716 both distinct and overlapping roles in meiotic recombination. *Genes Cells*
717 **2**, 615-629 (1997). https://doi.org:10.1046/j.1365-2443.1997.1480347.x
718 58 Bishop, D. K. RecA homologs Dmc1 and Rad51 interact to form multiple
719 nuclear complexes prior to meiotic chromosome synapsis. *Cell* **79**, 1081-
720 1092 (1994).
721 59 Chen, X. *et al.* Mek1 coordinates meiotic progression with DNA break
722 repair by directly phosphorylating and inhibiting the yeast pachytene exit
723 regulator Ndt80. *PLoS Genet* **14**, e1007832 (2018).
724 https://doi.org:10.1371/journal.pgen.1007832
725 60 Hollingsworth, N. M., Goetsch, L. & Byers, B. The HOP1 gene encodes a
726 meiosis-specific component of yeast chromosomes. *Cell* **61**, 73-84 (1990).
727 https://doi.org:10.1016/0092-8674(90)90216-2
728 61 Smith, A. V. & Roeder, G. S. The yeast Red1 protein localizes to the cores
729 of meiotic chromosomes. *J Cell Biol* **136**, 957-967 (1997).
730 https://doi.org:10.1083/jcb.136.5.957
731 62 Kniewel, R. *et al.* Histone H3 Threonine 11 Phosphorylation Is Catalyzed
732 Directly by the Meiosis-Specific Kinase Mek1 and Provides a Molecular
733 Readout of Mek1 Activity in Vivo. *Genetics* **207**, 1313-1333 (2017).
734 https://doi.org:10.1534/genetics.117.300359
735 63 Hollingsworth, N. M. & Gaglione, R. The meiotic-specific Mek1 kinase in
736 budding yeast regulates interhomolog recombination and coordinates
737 meiotic progression with double-strand break repair. *Curr Genet* **65**, 631-
738 641 (2019). https://doi.org:10.1007/s00294-019-00937-3
739 64 Alani, E., Padmore, R. & Kleckner, N. Analysis of wild-type and rad50

740 mutants of yeast suggests an intimate relationship between meiotic
741 chromosome synapsis and recombination. *Cell* **61**, 419-436 (1990).
742 https://doi.org:10.1016/0092-8674(90)90524-i
743 65 Usui, T., Ogawa, H. & Petrini, J. H. A DNA damage response pathway
744 controlled by Tel1 and the Mre11 complex. *Mol Cell* **7**, 1255-1266 (2001).
745 https://doi.org:10.1016/s1097-2765(01)00270-2
746 66 Zou, L. & Elledge, S. J. Sensing DNA damage through ATRIP recognition
747 of RPA-ssDNA complexes. *Science* **300**, 1542-1548 (2003).
748 https://doi.org:10.1126/science.1083430
749 67 Lin, Y. *et al.* APE1 recruits ATRIP to ssDNA in an RPA-dependent and -
750 independent manner to promote the ATR DNA damage response. *Elife* **12**
751 (2023). https://doi.org:10.7554/eLife.82324
752 68 Shinohara, M., Bishop, D. K. & Shinohara, A. Distinct Functions in
753 Regulation of Meiotic Crossovers for DNA Damage Response Clamp
754 Loader Rad24(Rad17) and Mec1(ATR) Kinase. *Genetics* **213**, 1255-1269
755 (2019). https://doi.org:10.1534/genetics.119.302427
756 69 Hustedt, N. *et al.* Yeast PP4 interacts with ATR homolog Ddc2-Mec1 and
757 regulates checkpoint signaling. *Mol Cell* **57**, 273-289 (2015).
758 https://doi.org:10.1016/j.molcel.2014.11.016
759 70 Li, K., Yoshimura, K. & Shinohara, M. Meiotic DNA double-strand break-
760 independent role of protein phosphatase 4 in Hop1 assembly to promote
761 meiotic chromosome axis formation in budding yeast. *Genes Cells* (2023).
762 https://doi.org:10.1111/gtc.13049
763 71 San-Segundo, P. A. & Roeder, G. S. Pch2 links chromatin silencing to
764 meiotic checkpoint control. *Cell* **97**, 313-324 (1999).
765 https://doi.org:10.1016/s0092-8674(00)80741-2
766 72 Borner, G. V., Barot, A. & Kleckner, N. Yeast Pch2 promotes domainal axis
767 organization, timely recombination progression, and arrest of defective
768 recombinosomes during meiosis. *Proceedings of the National Academy of*
769 *Sciences of the United States of America* **105**, 3327-3332 (2008).
770 https://doi.org:10.1073/pnas.0711864105
771 73 Herruzo, E. *et al.* The Pch2 AAA+ ATPase promotes phosphorylation of
772 the Hop1 meiotic checkpoint adaptor in response to synaptonemal
773 complex defects. *Nucleic Acids Res* **44**, 7722-7741 (2016).
774 https://doi.org:10.1093/nar/gkw506
775 74 Humphryes, N. *et al.* The Ecm11-Gmc2 complex promotes synaptonemal

complex formation through assembly of transverse filaments in budding yeast. *PLoS Genet* **9**, e1003194 (2013). https://doi.org:10.1371/journal.pgen.1003194

75 Lee, M. S. *et al.* The synaptonemal complex central region modulates crossover pathways and feedback control of meiotic double-strand break formation. *Nucleic Acids Res* **49**, 7537-7553 (2021). https://doi.org:10.1093/nar/gkab566

76 Shinohara, M., Gasior, S. L., Bishop, D. K. & Shinohara, A. Tid1/Rdh54 promotes colocalization of rad51 and dmc1 during meiotic recombination. *Proceedings of the National Academy of Sciences of the United States of America* **97**, 10814-10819 (2000). https://doi.org:10.1073/pnas.97.20.10814

77 Shinohara, M., Oh, S. D., Hunter, N. & Shinohara, A. Crossover assurance and crossover interference are distinctly regulated by the ZMM proteins during yeast meiosis. *Nat Genet* **40**, 299-309 (2008). https://doi.org:10.1038/ng.83

78 Bani Ismail, M., Shinohara, M. & Shinohara, A. Dot1-dependent histone H3K79 methylation promotes the formation of meiotic double-strand breaks in the absence of histone H3K4 methylation in budding yeast. *PLoS One* **9**, e96648 (2014). https://doi.org:10.1371/journal.pone.0096648

798 **Figure legends**

799

800 **Figure 1. A pathway of recombination checkpoint in meiosis.**

801

802 **Figure 2. Rfa1 depletion alleviates *dmc1*-induced pachytene arrest**

803 (A) Expression of various proteins in meiosis. Lysates obtained from the *dmc1*
804 *RFA1-AID* (SAY63/64) cells at various time points during meiosis with or
805 without the addition of auxin at 4 h were analyzed by western blotting using
806 anti-myc (Rfa1-myc-AID, upper), anti-Hop1, anti-histone H3-phospho-T11,
807 anti-Ndt80, anti-Cdc5 or anti-tubulin (lower) antibodies.

808 (B) Rfa2 staining. Nuclear spreads from *dmc1 RFA1-AID* (SAY63/64) cells with
809 or without the addition of auxin at 4 h were stained with anti-Rfa2 (red), and
810 DAPI (blue). Representative images at each time point under the two
811 conditions are shown. Bar = 2 μm.

812 (C) Kinetics of Rfa2 assembly/disassembly. The number of Rfa2-positive cells
813 (with more than 5 foci) was counted at each time point. At each time point,
814 more than 100 cells were counted.

815 (D) Meiotic cell cycle progression. The entry into meiosis I and II in *dmc1 RFA1-*
816 *AID* (SAY63/64) cells were analyzed by DAPI staining. The number of DAPI
817 bodies in a cell was counted. A cell with 2, 3, and 4, and 3 and 4 DAPI bodies
818 was defined as a cell that passed through meiosis I and meiosis II,
819 respectively. The graph shows the percentages of cells that completed MI or
820 MII at the indicated time points. More than 200 cells were counted at each
821 time point. The representative results (n=3) are shown. *dmc1 RFA1-AID*
822 without auxin, blue closed circles; *dmc1 RFA1-AID* with auxin addition at 4 h,
823 red closed circles.

824 (E) FACS profile of the *dmc1 RFA1-AID* mutant without or with auxin addition at
825 4 h. Fixed cells at each time point were stained with PI and analyzed by FACS
826 cell sorter.

827 (F) Tubulin staining in the *dmc1 RFA1-AID* mutant. Whole cells were fixed and
828 stained with anti-tubulin (green) and DAPI (blue). Representative images for
829 each class are shown. Bar = 2 μm.

830 (G) Whole cells were fixed and stained with anti-tubulin (green) and DAPI (blue).
831 Representative images at 8 h of *dmc1 RFA1-AID* (SAY63/64) cells with or
832 without the addition of auxin at 4 h are shown. Bar = 2 μm.

833 (H) Classification of tubulin staining at each time point of meiosis in *dmc1 RFA1-*

834 *AID* (SAY63/64) cells with (right) or without (left) the addition of auxin at 4 h.
835 Dot, short line, and long line tubulin-staining with single DAPI mass were
836 defined as prophase I (blue), metaphase I (red), anaphase I (orange),
837 metaphase II (blue), anaphase II (green) and post-meiosis II (pale green).
838 Short and long tubulin-staining were defined as metaphase II and anaphase
839 II, respectively. At each time point, more than 100 cells were counted. The
840 representative results are shown (*n*=3).
841
842 **Figure 3. Rfa1 depletion does not affect DSB turnovers in *dmc1* mutant**
843 (A) CHEF analysis of meiotic DSB repair. Chromosomal DNAs from *dmc1 RFA1-*
844 *AID* (SAY63/64) cells with or without the addition of auxin at 4 h were studied
845 by CHEF electrophoresis. Auxin was added at 4 h in the incubation with SPM.
846 (B) Rad51 staining. Nuclear spreads from *dmc1 RFA1-AID* (SAY63/64) cells with
847 or without the addition of auxin at 4 h were stained with anti-Rad51 (red), and
848 DAPI (blue). Representative images at each time point under the two
849 conditions are shown. Bar = 2 μm.
850 (C) Kinetics of Rad51 assembly/disassembly. The number of Rad51-positive cells
851 (with more than 5 foci) was counted at each time point. At each time point,
852 more than 100 cells were counted.
853 (D) Hop1 staining. Nuclear spreads from *dmc1 RFA1-AID* (SAY63/64) cells with
854 or without the addition of auxin at 4 h were stained with anti-Hop1 (red), and
855 DAPI (blue). Representative images at each time point under the two
856 conditions are shown. Bar = 2 μm.
857 (E) Kinetics of Hop1 assembly/disassembly. The number of Rad51-positive cells
858 (with more than 5 foci) was counted at each time point. At each time point,
859 more than 100 cells were counted.
860
861 **Figure 4. *NDT80* is necessary for pachytene exit by Rfa1 depletion**
862 (A) Expression of various protein in meiosis. Lysates obtained from the *ndt80*
863 *dmc1 RFA1-AID* (SAY80/81) cells at various time points during meiosis with
864 or without the addition of auxin at 4 h were analyzed by western blotting using
865 anti-myc (Rfa1-myc-AID, upper), anti-Hop1, anti-Cdc5 or anti-tubulin (lower)
866 antibodies.
867 (B) Rfa2 staining. Nuclear spreads from *ndt80 dmc1 RFA1-AID* (SAY80/81) cells
868 with or without the addition of auxin at 4 h were stained with anti-Rfa2 (red),
869 and DAPI (blue). Representative images at each time point under the two

870 conditions are shown. Bar = 2 μm.
871 (C) Classification of tubulin staining at each time point of meiosis in *ndt80 dmc1*
872 *RFA1-AID* (SAY80/81) cells with (right) or without (left) the addition of auxin at
873 4 h. Dot, short line, and long line tubulin-staining with single DAPI mass were
874 defined as prophase I (blue), metaphase I (red), anaphase I (orange),
875 metaphase II (blue), anaphase II (green) and post-meiosis II (pale green).
876 Short and long tubulin-staining were defined as metaphase II and anaphase
877 II, respectively. At each time point, more than 100 cells were counted. The
878 representative results are shown (*n*=2).
879 (D) Hop1 staining. Nuclear spreads from *ndt80 dmc1 RFA1-AID* (SAY SAY80/81)
880 cells with or without the addition of auxin at 4 h were stained with anti-Hop1
881 (red), and DAPI (blue). Representative images at each time point under the
882 two conditions are shown. Bar = 2 μm.
883
884 **Figure 5. Rfa1 depletion alleviates *zip1*-induced delay in meiosis I**
885 (A) Expression of various protein in meiosis. Lysates obtained from the *zip1*
886 *RFA1-AID* (SAY72/73) cells at various time points during meiosis with or
887 without the addition of auxin at 4 h were analyzed by western blotting using
888 anti-myc (Rfa1-myc-AID, upper), anti-Hop1, anti-Cdc5, anti-histone H3-
889 phospho-T11 or anti-tubulin (lower) antibodies.
890 (B) Meiotic cell cycle progression. The entry into meiosis I and II in *zip1 RFA1-*
891 *AID* (SAY72/73) cells were analyzed by DAPI staining as shown in Figure 1D.
892 More than 200 cells were counted at each time point. The representative
893 results (*n*=3) are shown. *dmc1 RFA1-AID* without auxin, blue closed circles;
894 *dmc1 RFA1-AID* with auxin addition at 4 h, red closed circles.
895 (C) Rfa2 staining. Nuclear spreads from *zip1 RFA1-AID* (SAY72/73) cells with or
896 without the addition of auxin at 4 h were stained with anti-Rfa2 (red), and DAPI
897 (blue). Representative images at each time point under the two conditions are
898 shown. Bar = 2 μm.
899 (D) Tubulin staining in the *zip1 RFA1-AID* mutant. Whole cells were fixed and
900 stained with anti-tubulin (green) and DAPI (blue). Representative images for
901 each class are shown. Bar = 2 μm.
902 (E) Classification of tubulin staining at each time point of meiosis in *zip1 RFA1-*
903 *AID* (SAY72/73) cells with (right) or without (left) the addition of auxin at 4 h.
904 The quantification was performed as shown in Figure 1G. At each time point,
905 more than 100 cells were counted. The representative results are shown (*n*=2).

906 (F) Hop1 staining. Nuclear spreads from *zip1 RFA1-AID* (SAY72/73) cells with or
907 without the addition of auxin at 4 h were stained with anti-Hop1 (red), and
908 DAPI (blue). Representative images at each time point under the two
909 conditions are shown. Bar = 2 μm.
910 (G) CHEF analysis of meiotic DSB repair. Chromosomal DNAs from *zip1 RFA1-*
911 *AID* (SAY72/73) cells with or without the addition of auxin at 4 h were studied
912 by CHEF electrophoresis. Auxin was added at 4 h in the incubation with SPM.
913 (H) Kinetics of assembly/disassembly of Rfa2, Rad51, and Hop1. The number of
914 focus-positive cells (with more than 5 foci) was counted at each time point. At
915 each time point, more than 100 cells were counted.
916
917 **Figure 6. Rfa1 depletion does not suppress *rad50S*-induced delay in**
918 **meiosis I**
919 (A) Expression of various proteins in meiosis. Lysates obtained from the *rad50S*
920 *RFA1-AID* (SAY68/69) cells at various time points during meiosis with or
921 without the addition of auxin at 4 h were analyzed by western blotting using
922 anti-myc (Rfa1-myc-AID, upper), anti-Hop1, anti-Cdc5 or anti-tubulin (lower)
923 antibodies.
924 (B) Classification of tubulin staining at each time point of meiosis in *rad50S RFA1-*
925 *AID* (SAY68/69) cells with (right) or without (left) the addition of auxin at 4 h.
926 The quantification was performed as shown in Figure 1G. At each time point,
927 more than 100 cells were counted. The representative results are shown (n=1).
928 (C) CHEF analysis of meiotic DSB repair. Chromosomal DNAs from *zip1 RFA1-*
929 *AID* (SAY68/69) cells with or without the addition of auxin at 4 h were studied
930 by CHEF electrophoresis. Auxin was added at 4 h in the incubation with SPM.
931 (D) Rfa2 staining. Nuclear spreads from *rad50S RFA1-AID* (SAY68/69) cells with
932 or without the addition of auxin at 4 h were stained with anti-Rfa2 (red), and
933 DAPI (blue). Representative images at each time point under the two
934 conditions are shown. Bar = 2 μm.
935 (E) Hop1 staining. Nuclear spreads from *rad50S RFA1-AID* (SAY68/69) cells with
936 or without the addition of auxin at 4 h were stained with anti-Hop1 (red), and
937 DAPI (blue). Representative images at each time point under the two
938 conditions are shown. Bar = 2 μm.
939
940 **Supplemental Figure S1.**
941 (A) The number of Rfa2 foci per spread in *dmc1 RFA1-AID* (SAY72/73) cells with

942 (red) or without (blue) the addition of auxin at 4 h was counted at different time
943 points. The mean and SD are shown in the plot.
944 (B) The number of Rad51 foci per spread *dmc1 RFA1-AID* (SAY72/73) cells with
945 (red) or without (blue) the addition of auxin at 4 h was counted at different time
946 points. The mean and SD are shown in the plot.
947 (C) The number of Rfa2 foci per spread in *zip1 RFA1-AID* (SAY72/73) cells with
948 (red) or without (blue) the addition of auxin at 4 h was counted at different time
949 points. The mean and SD are shown in the plot.
950 (D) The number of Rad51 foci per spread *zip1 RFA1-AID* (SAY72/73) cells with
951 (red) or without (blue) the addition of auxin at 4 h was counted at different time
952 points. The mean and SD are shown in the plot.
953
954 **Supplemental Figure S 2.**
955 CHEF analysis of meiotic DSB repair. Chromosomal DNAs from Wild type
956 (MSY831/833) and the *dmc1* mutant cells were studied by CHEF electrophoresis.
957 Auxin was added at 4 h in the incubation with SPM.
958

959 **Supplementary Information**

960 **Table S1. Strain List**

Strain number	Genotypes
MSY831/833	*MAT**a**/ α, ho::LYS2/", lys2/", ura3/", leu2::hisG/", trp1::hisG/"*
NKY1551	*MAT**a**/ α, ho::LYS2/", lys2/", ura3/", leu2::hisG/", his4X-LEU2(BamHI)-URA3/his4B-LEU2(MluI), arg4-bgl/arg4-nsp*
SAY15/16	MSY831/833 with *Rfa1-AID::HYG/", p-CUP1-Os-Tir1::URA3*
SAY63/64	SAY15/16 with *dmc1::URA3/"*
SAY68/69	SAY15/16 with *rad50S::LEU2/"*
SAY72/73	SAY15/16 with *zip1::LEU2/"*
SAY80/81	SAY15/16 with *ndt80::LEU2/"*

961

962 **Table S2. Oligonucleotide list**

963 **Table S2. Primer List**

Primer name	Sequence
Rfa1-AID-Hygro-F	5'-TTG AAT TAC AGG GCT GAA GCC GAC TAT CTT GCC GAT GAG TTA TCC AAG GCT TTG TTA GCT CGT ACG CTG CAG GTC GAC
Rfa1-AID-Hygro-R	5'-TTT TTT TTT TAC ATT TCT CAT ATG TTA CAT AGA TTA AAT AGT ACT TGA TTA TTT GAT ACA ATC GAT GAA TTC GAG CTC G
RFA1-F	5'-GTG AGA AGT GCG ACA CCA ATA
RFA1-R	5'-GTC GAC TAT TTG GAG AAG GAA G

964

965

Figure 1. Arivarasan S. et al.

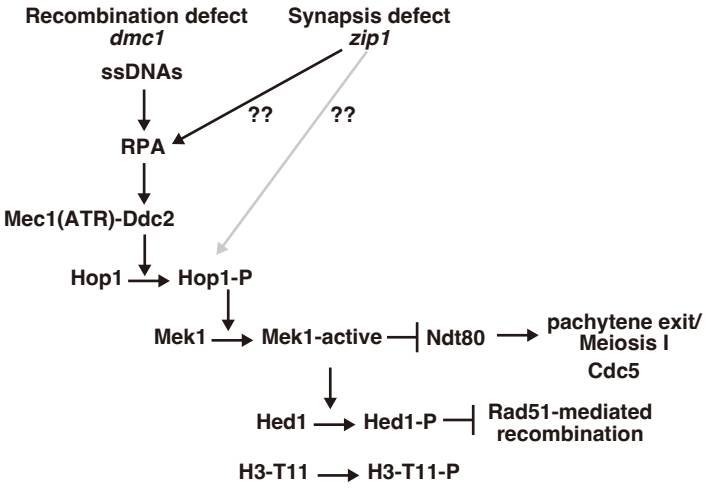

Figure 2. Arivarasan S. et al.

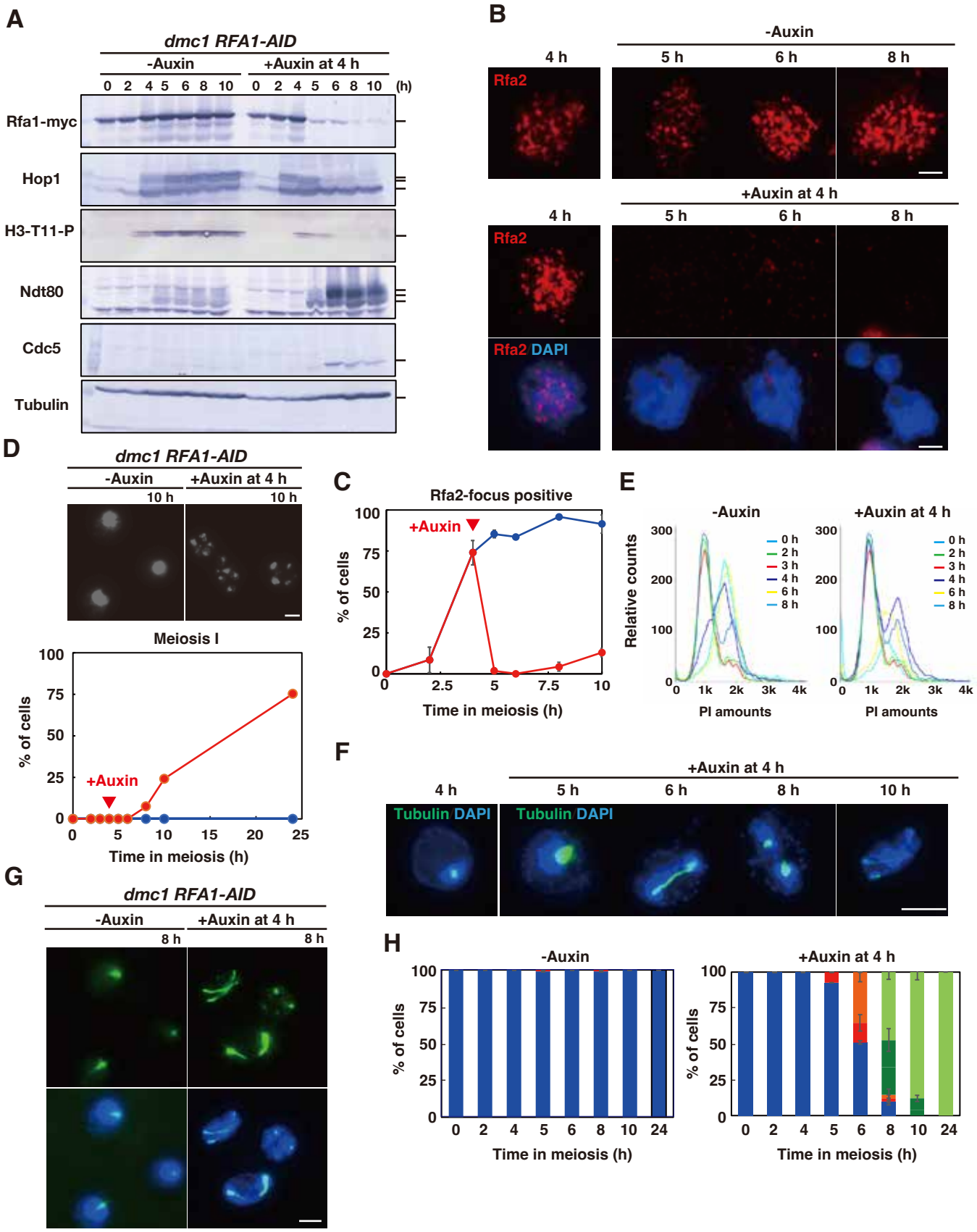

Figure 3. Arivarasan S. et al.

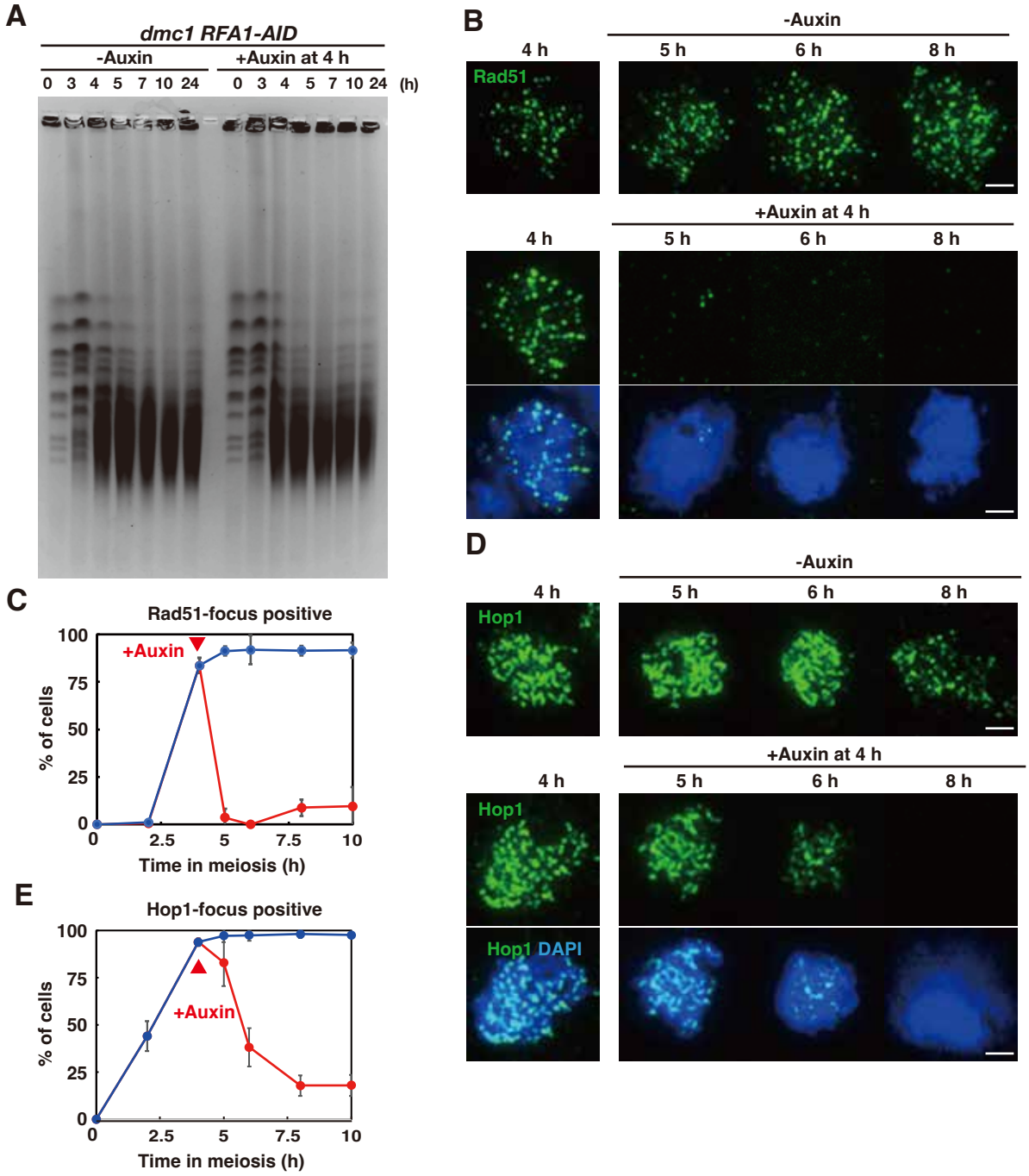

Figure 4. Arivarasan S. et al.

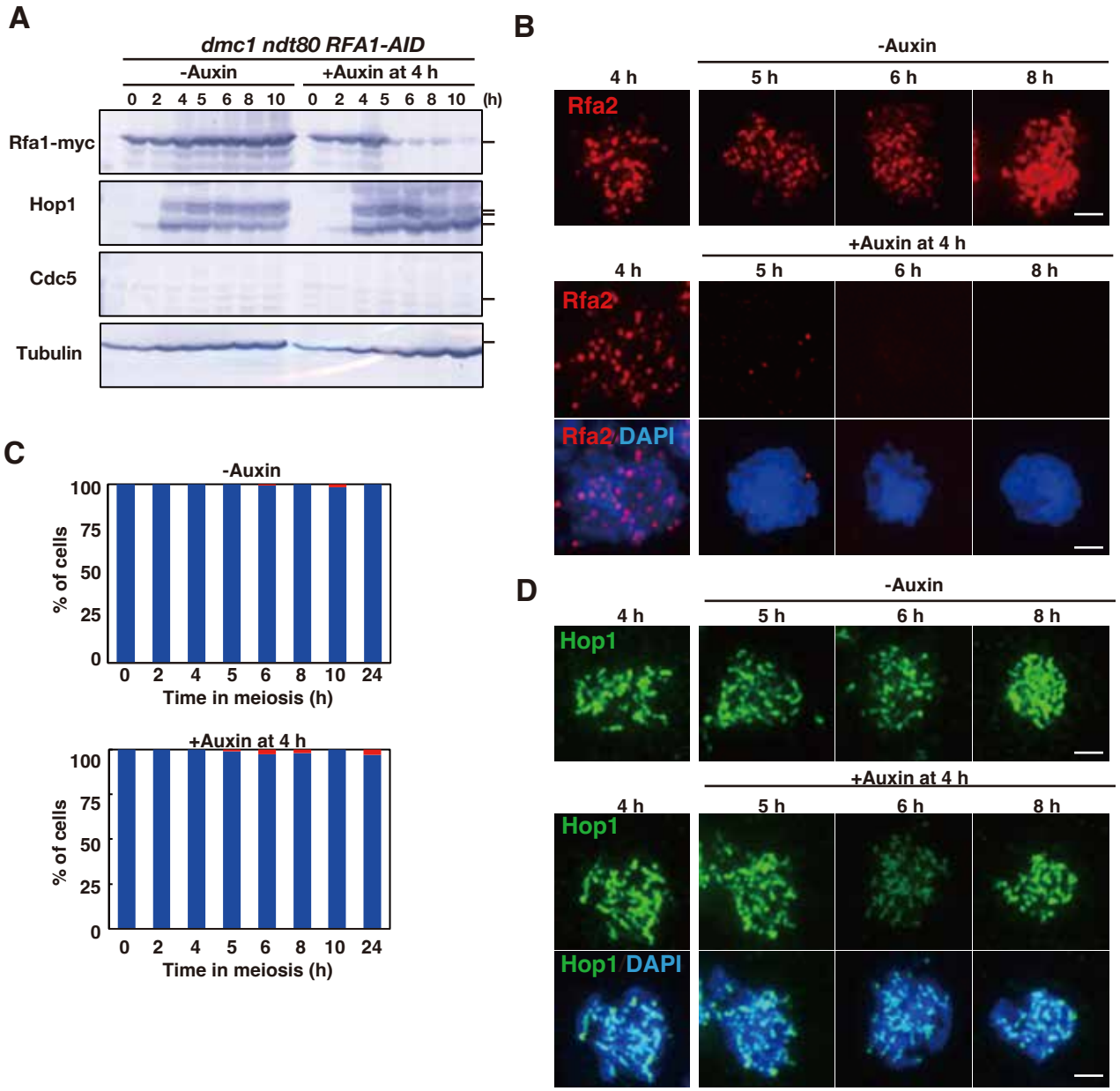

Figure 5. Arivarasan S. et al.

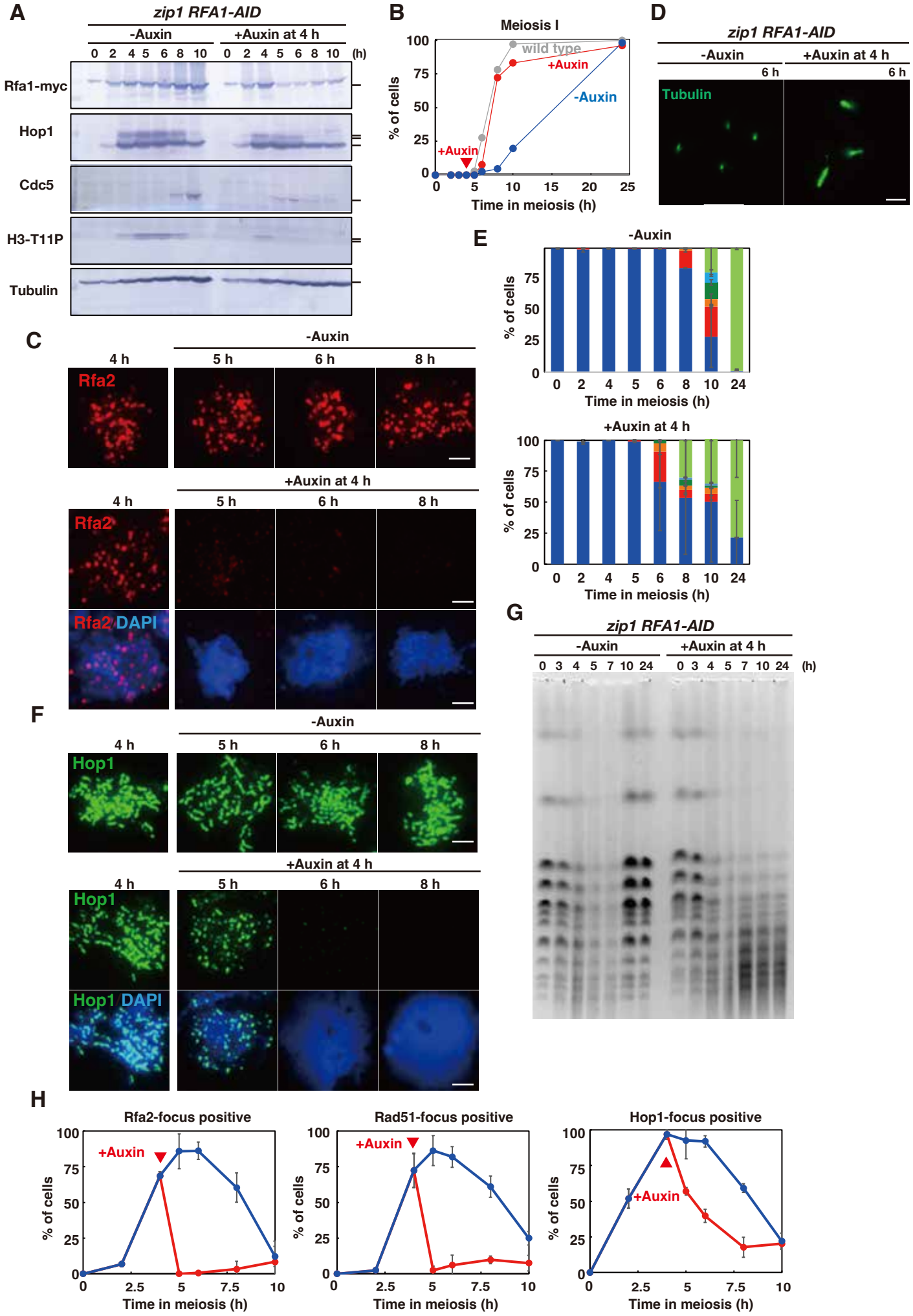

Figure 6. Arivarasan S. et al.

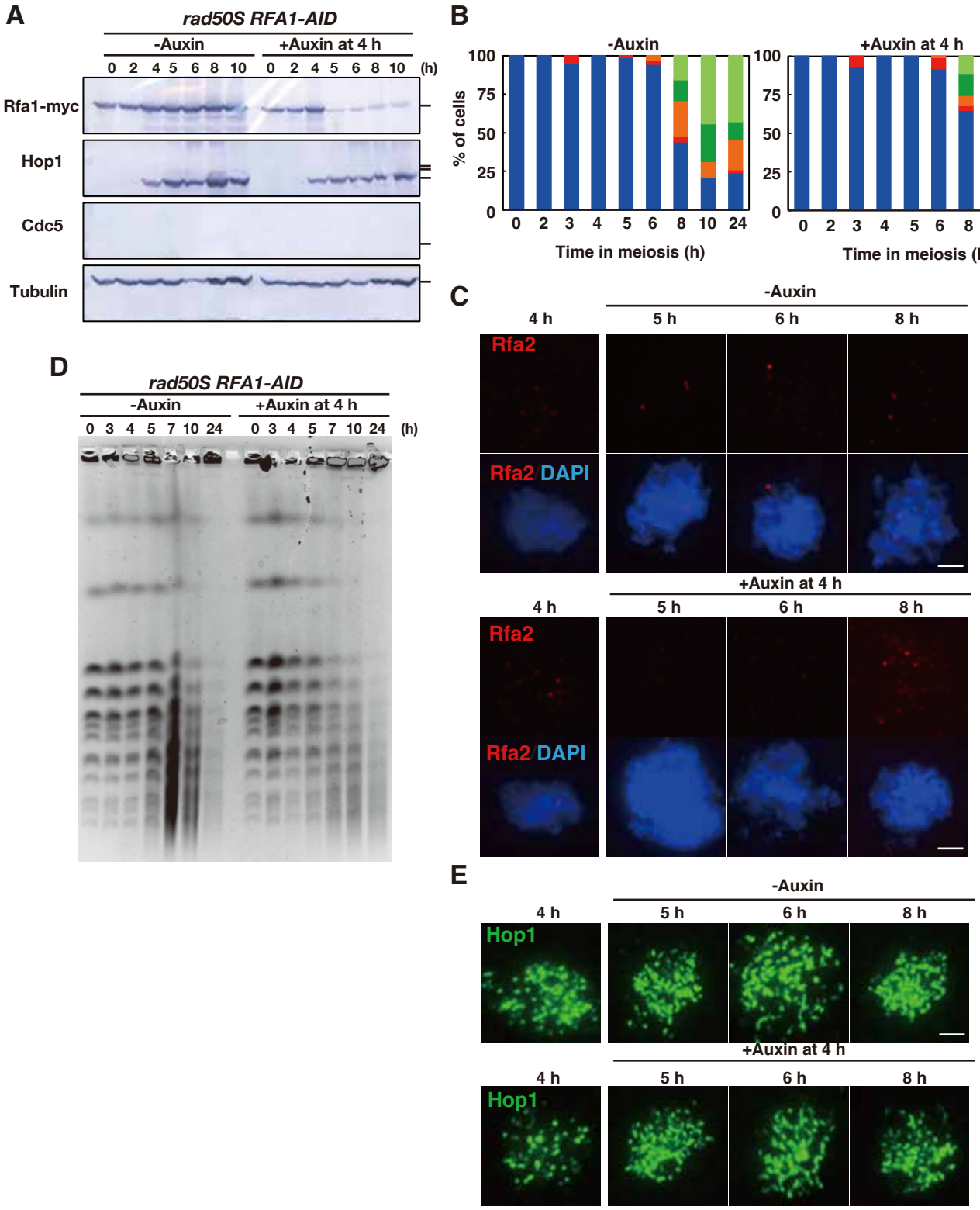

Supplementary Figure S1. Arivarasan S. et al.

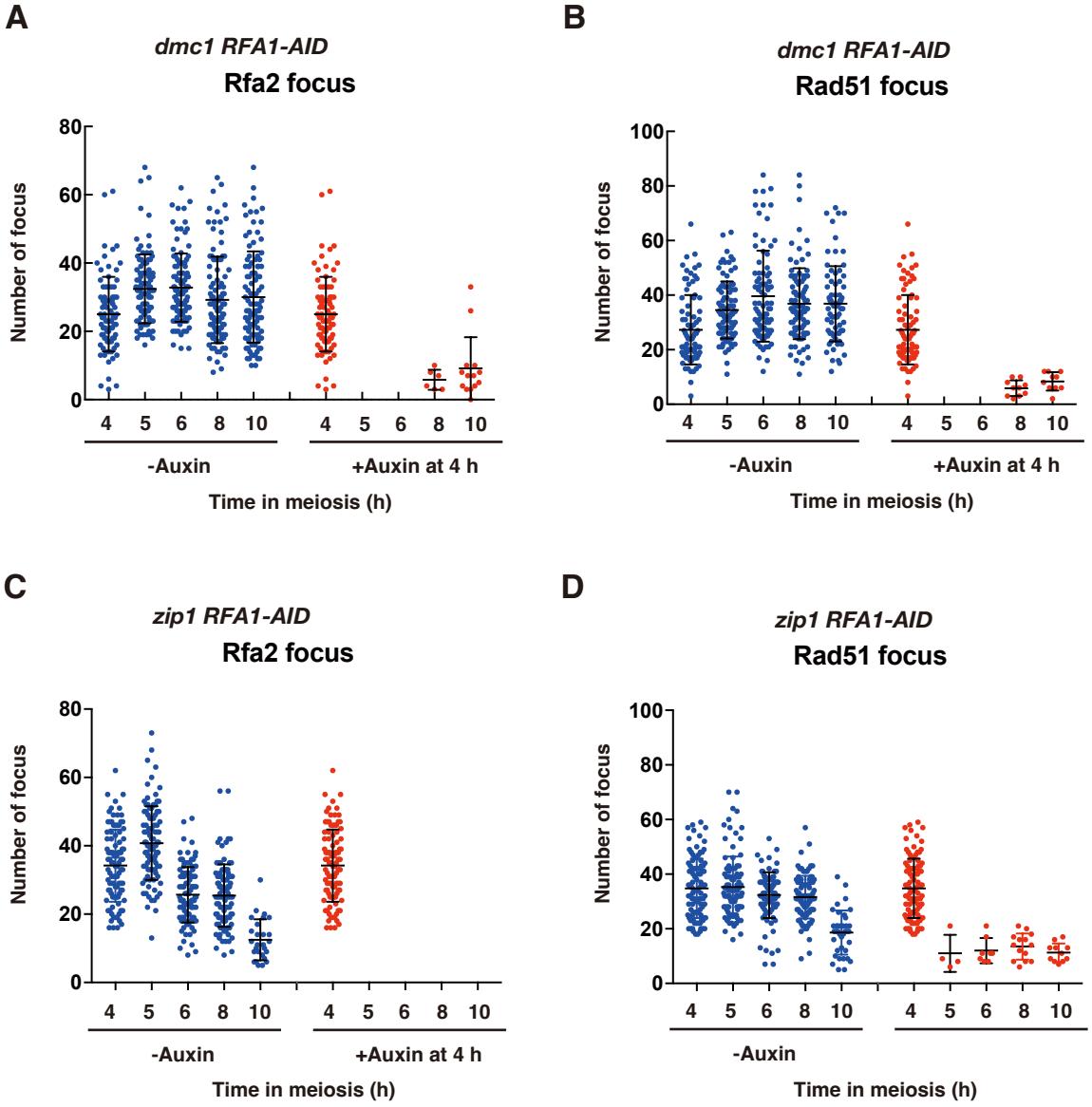
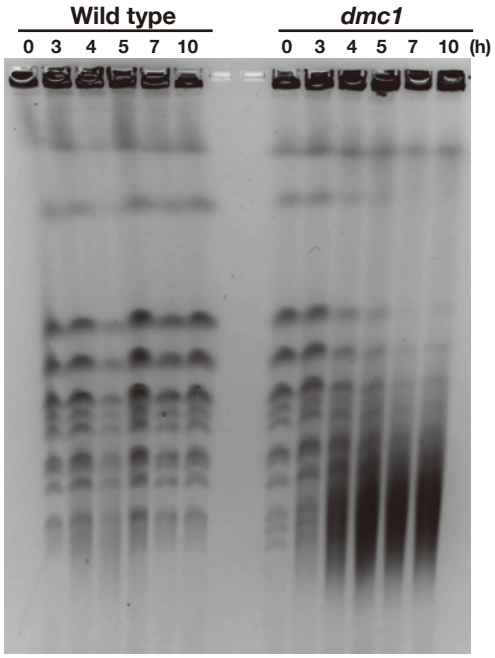
Supplementary Figure S2. Arivarasan S. et al.